

Combined Experimental and Quantum Chemical Investigation of Chiroptical Properties of Nicotinamide Derivatives with and without Intramolecular Cation– π Interactions

Akinori Shimizu,[†] Tadashi Mori,^{*,†} Yoshihisa Inoue,^{*,†} and Shinji Yamada[‡]

Department of Applied Chemistry, Graduate School of Engineering, Osaka University, 2-1 Yamada-oka, Suita 565-0871, Japan, and Department of Chemistry, Graduate School of Science, Ochanomizu University, Tokyo 112-8610, Japan

Received: May 6, 2009; Revised Manuscript Received: June 10, 2009

The circular dichroism (CD) spectra of neutral and cationic nicotinamide derivatives were experimentally examined in solution and in the solid state to show dramatic differences in the two phases and appreciable dependence on temperature and solvent. The CD spectrum of neutral nicotinamide **1** in solution was reproduced theoretically by averaging the theoretical spectra calculated for all of the extended and folded conformers (*s-trans-G*⁺, *s-cis-G*⁺, *s-trans-T*, and *s-cis-T*) weighted by their population. The preference for the folded, over the extended, conformers in less polar solvent was indicated by the calculation and confirmed experimentally by the analysis of specific rotations. Theoretical CD spectrum calculated for the conformer found in the X-ray structural analysis (*s-cis-T*) well reproduced the experimental CD spectrum measured in the solid state. Introducing cation– π interactions by *N*-methylation of **1** to give **1-Me**⁺ led to dramatic changes in CD spectrum. Nevertheless, the experimental CD spectrum of **1-Me**⁺ was well reproduced by averaging the theoretical spectra calculated for a pair of most stable conformers (*s-cis-G*⁺ and *s-trans-G*⁺) of **1-Me**⁺. The CD spectrum calculated for the *s-trans-G*⁺ conformer, which was found in the X-ray crystallographic analysis, did not agree with the experimental one. The theoretical spectra were better reproduced in general by the more sophisticated RI-CC2 method, but the conventional TD-DFT method also gave acceptable results. This allowed us to successfully calculate the larger derivative **2-Me**⁺, for which the RI-CC2 method was not practically applicable. These results show that the structure/conformation may vary with the conditions employed (e.g., by altering the solvent or phase) and thus the experimental analysis under the identical condition is essential for a serious structural study. The present study on a series of nicotinamide derivatives **1**, **1-Me**⁺, and **2-Me**⁺ with and without cation– π interactions demonstrates that the combination of experimental and theoretical chiroptical methods is capable of providing reliable structural/conformational information in solution phase, which is complementary to the X-ray crystallographic structure in the solid state.

Introduction

As a consequence of the recent advances in quantum chemical calculations, especially the time-dependent (linear-response) density functional theory (TD-DFT),¹ chiroptical properties of small molecules have become being easily calculated. The popular TD-DFT method has been widely employed as a tool for determining the absolute configuration of unassigned chiral molecules and also for better understanding the chiroptical properties. Among the several chiroptical properties such as optical rotatory dispersion, vibrational circular dichroism,² and electronic circular dichroism (CD),³ the electronic CD has been increasingly recognized as a powerful means for analyzing the conformational behavior in solution. We⁴ and others⁵ have recently reported the combined experimental and theoretical CD spectral studies applied to the elucidation of conformation (and configuration) of relatively large chiral molecules. The theoretical spectra calculated for such systems have been used mostly as supplementary information to reinforce the conformational (and configurational) predictions. Such chiroptical methods, however, have not been exploited in the examination of intramolecular noncovalent interactions.

In the present study, we wish to demonstrate how the combined use of experimental and theoretical chiroptical analyses is useful (and reliable) for elucidating and discussing the structural and conformational behavior in solution, by using a series of nicotinamide derivatives **1**, **1-Me**⁺, and **2-Me**⁺ (Chart) as a challenging target system that incorporates the cation– π interaction. We chose these nicotinamide derivatives, because the X-ray crystal structures (of both neutral and cationic species) are known,⁶ and the conformational (structural) variation can be easily achieved by using different solvents and/or temperatures. Additionally, introducing a cation– π interaction may lead to significant changes in conformation and therefore in chiroptical properties, which can be used in turn as a probe for the conformational changes of the molecule in solution.

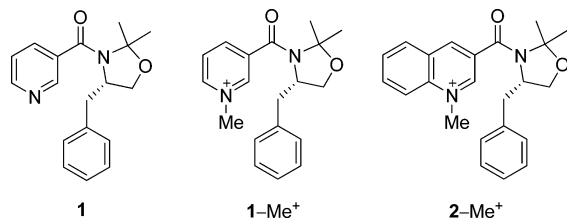
1. Chiral Nicotinamide **1** and the Related Cationic Species **1-Me**⁺ and **2-Me**⁺

Noncovalent interactions play a dominant role in vast areas of current chemistry, ranging from the supramolecular recognition in molecular biology to the construction of sophisticatedly designed architectures in materials science and technology. Cation– π interaction⁷ has now been accepted and well recognized as one of such important interactions, but the significance and applicability of this binding mode have been extensively studied only recently. This interaction

* To whom correspondence should be addressed. Fax: +81-6-6879-7923. E-mail: tmori@chem.eng.osaka-u.ac.jp.

[†] Osaka University.

[‡] Ochanomizu University.



was initially recognized in protein crystal structures,⁸ but was also revealed experimentally in the gas phase⁹ as well as in the condensed phase,¹⁰ and also has become studied by theory.¹¹ Cation- π interactions are not limited to the (alkali) metal cation- π ;¹² the interaction between an organic cation (pyridinium, quinolinium, etc.) and an aromatic system has been successfully applied to the control of stereo(regio)selective thermal¹³ as well as photochemical¹⁴ reactions. Traditionally, this type of interaction was considered as donor-acceptor in nature,¹⁵ but the recent theoretical investigation based on the CCSD(T) calculations has clearly demonstrated that the donor-acceptor interaction plays a minor role but the cation- π interaction is the major contributor to the stability of such a system.¹⁶

Although reactions are usually performed in solution, the reactivity, selectivity, and/or mechanism are frequently discussed based on the X-ray crystal structures of relevant reactants, products, and reactive intermediates isolated, and the conclusions derived therefrom are accepted in most of the cases.¹⁷ Indeed, successful isolation of reactive radical cations¹⁸ and ions¹⁹ involved in electrophilic reactions as intermediates allows us to speculate on the plausible reaction mechanisms and rationalize the selectivities of the reactions in solution. Nevertheless, X-ray structure sometimes fails to account for the stereoselectivities of the reaction, thus indicating that the structures in solution have to be considered significantly different from the crystal structures. As mentioned above, the X-ray crystal structure of **1-Me⁺** has been already determined.⁶ Accordingly, the cation- π interaction between the pyridinium and the benzene ring has been established for this nicotinamide derivative by the observation of the folded conformation, in which two aromatic planes are arranged face-to-face with a separation of ~ 3.4 Å. However, this structure does not appear to be kept in the solution phase, since the stereoselectivity observed in the nucleophilic reaction of an analog of **1-Me⁺** (**1-CO₂Me⁺**) indicated that the nucleophiles attack occurs from the B-side (and the cation- π interaction on the A-side²⁰ of the pyridinium ring), which is completely opposite to the X-ray structure. The solution-phase structures of the molecule has been also studied by the use of spectroscopic (e.g., EPR, 2D-NMR, and fluorescence) techniques,²¹ applicability of which is however rather limited and specific to each system. Herein, we will show the validity and advantages of a combined experimental and theoretical CD spectral study,²² by demonstrating that the dominant structures in solution are different from the crystal structures in both neutral and cationic nicotinamides. A successful reproduction of the CD spectra in solution by theory will reveal the calculated energies of conformers and their population to be reliable, which will be further supported by the comparison of the experimental and theoretical specific rotations. Although the cation- π interaction has been revealed by X-ray structural analysis, the real conformations existing in the solution phase (where reaction occurs) can be elucidated only by using the chiroptical method.

Experimental Section

Reinvestigation of the Experimental CD Spectra of Nicotinamide Derivatives. The experimental CD spectra were obtained for 30 μ M solutions of **1**, **1-Me⁺Br⁻**, and **2-Me⁺Br⁻** in acetonitrile, methanol, dichloromethane, or methylcyclohexane, with a conventional 1-cm quartz cell at temperatures ranging from +25 to -75 °C with a Unisoku cryostat (conditions: response 4 s; bandwidth 2 nm; scan rate 100 nm min⁻¹). The solid-state CD spectra were obtained for KBr disks at an ambient temperature (~ 20 °C). To confirm the absence of linear dichroism and other artifacts, eight measurements were made by rotating the disk by 90° and by alternating the disk face) to give practically the identical spectra, all of which were averaged.

Quantum Chemical Computations. All calculations were performed on Linux-PCs using the TURBOMOLE 5.9 program suite.²³ All geometry optimizations were performed at the dispersion-corrected DFT-D-B-LYP level without any symmetry constraint (C_1) with a numerical quadrature multiple grid of m4.²⁴ All possible conformations were considered and calculated with an AO basis set of valence double- ζ quality with polarization function, termed as the basis-set SV(P). The conformations with relative energies of up to 6 kcal mol⁻¹ were then fully optimized at the same level of theory with a larger basis-set TZV2P (in standard notation: H, [3s2p], C/N/O, [5s3p2d], which is an AO basis set of valence triple- ζ quality with two sets of polarization functions). Then, the minor conformers with relative energies larger than 3 kcal mol⁻¹ at this level were disregarded. The resolution of identity (RI) approximation²⁵ was employed in all DFT-D-B-LYP calculations, and the corresponding auxiliary basis sets were taken from the TURBOMOLE basis-set library. Details of conformer considerations are reported in the Supporting Information (SI). Subsequent single-point energy calculations were performed by the SCS-MP2 method with a TZVPP basis-set that has additional d/f and p/d functions on non-hydrogen and hydrogen atoms, respectively.²⁶ The SCS-MP2 method is a simple and logical amendment of the MP2 scheme, where the correction is made on the basis of a different scaling of the same-spin (E_{SS}) and opposite-spin (E_{OS}) electron pair contributions to the correlation energy (scaling factors are 6/5 and 1/3, respectively). The method is expected to provide the most accurate relative energies comparable to the computationally highly demanding CCSD(T) calculations, and thus used to obtain the final Boltzmann distribution at 298 K of the conformers. The relative energies of the DFT-D method were turned out to be comparable to the SCS-MP2 energies, which contrasts to the results obtained with the standard DFT method.²⁷ The effect of the solvent on the conformer distribution was also evaluated by using the PCM model. Thus, single-point energy calculations were performed with conductor-like screening model (COSMO)²⁸ as implemented in the TURBOMOLE program suite. The dielectric constant (ϵ) of 36.64 in acetonitrile and optimized atomic radii for the construction of the molecular cavity (C, 2.00; N, 1.83; O, 1.72; H, 1.30 Å) were used.

All excited-state calculations were performed with the optimized ground-state geometries, which means the vertical transition or the Franck-Condon states. The CD and UV-vis spectra of **1**, **1-Me⁺**, and **2-Me⁺** were first simulated on the basis of time-dependent density functional theory (TD-DFT)²⁹ with the BH-LYP³⁰ functional and employing the TZV2P basis set, which have been proven to be very successful for the previous systems.⁴ The spectra of **1** and **1-Me⁺** were also calculated by the resolution of the identity, time-dependent coupled cluster (RI-CC2) method³¹ with the TZVPP basis set, in order to verify

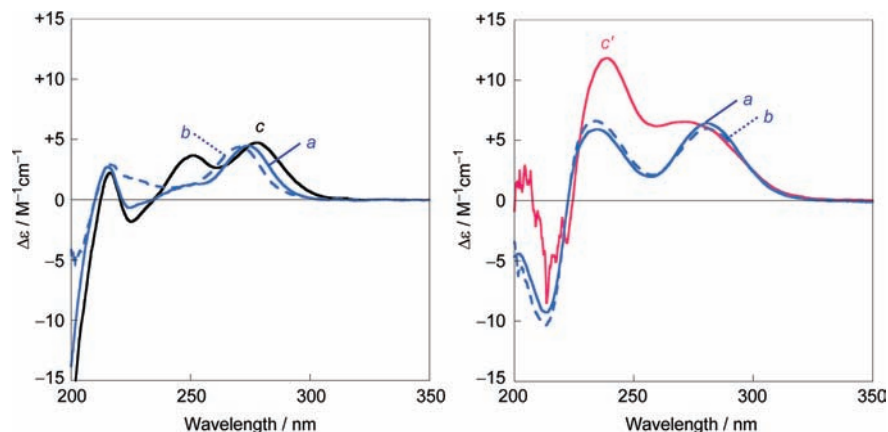


Figure 1. CD spectra of **1** (left) and **1-Me⁺** (right) (a) in acetonitrile, (b) in methanol, (c) in methylcyclohexane, or (c') in dichloromethane at 25 °C.

the applicability and accuracy of the less costly TD-DFT method for these nicotinamide systems. The program modules *escf*³² and *ricc2*³³ were used in the TD-DFT and RI-CC2 treatment, respectively. The calculated optical rotatory strengths can only be compared with the experimental values when they are origin-independent, but with our relatively large triple- ζ type AO basis-sets, the length and velocity rotational strengths converge to almost the same value, which indicates sufficient basis set saturation (differences are mostly less than a few %). In the present study, we chose the values from the reportedly robust length-gauge representations for the rotatory and oscillator strengths. The CD spectra were simulated by overlapping Gaussian functions for each transition where the width of the band at $1/e$ height is fixed at 0.4 eV. The resulting intensities of the combined spectra in the TD-DFT treatments were scaled to 1/2 to fit to the experimental values. The intensities obtained by the RI-CC2 treatments were not scaled. The excitation energies can be approximately identified as the band maxima in the experimental spectra. Due to the systematic errors of the theoretical transition energies compared to the experimental ones, the spectra were uniformly shifted so as to match to the maximal CD intensities, and the shift values are indicated in the caption of each Figure. The optical (specific) rotations at the sodium-D line wavelength (589 nm) were also calculated at the TD-DFT method with BH-LYP or B3-LYP functional and with Dunning's³⁴ aug-cc-pVDZ, aug-cc-pVTZ, or aug-SVP basis-set for the same optimized structures.

Results and Discussion

Experimental Circular Dichroism of Nicotinamide **1 and Its Cation- π Derivative **1-Me⁺**. a. *Solvent-Dependence.* The electronic absorption and circular dichroism (CD) spectra of chiral nicotinamide **1** were previously studied in some detail in acetonitrile.³⁵ The observed difference in CD spectra between neutral species and its cationic derivative was substantial, suggesting that the latter species was conformationally restrained due to the cation- π interaction. Although such interactions between the pyridinium moiety and benzene ring might be definitive, we examined the CD spectra in further detail, since (1) the previous explanation of the conformations of **1** and **1-Me⁺** was solely based on the empirical exciton chirality rule, but we would like to clarify the effect of the cation- π interactions on the validity of such empirical assessment; (2) by incorporating the recent advances in quantum chemical calculations, one can assess more detailed conformational information and presumably estimate the possible conforma-**

tional contributions of the relevant species in solution; and (3) the spectra were recorded only in polar acetonitrile and the effect of solvent has not been examined. The conformation, and in particular the CD spectrum, of the cationic species, are suspected to be significantly affected by solvation in acetonitrile. It is more suitable to compare the theoretical spectra (in gas phase) with those taken in less solvating (thus less polar) solvents.

Figure 1 (left) shows the experimental CD spectra of **1** in a variety of solvents at 25 °C. The spectra were largely dependent on the solvent used. The first band in the 260–300 nm region can be assigned to the local π - π^* transition of the pyridine moiety (see Tables S5 and S6 in SI). The positive Cotton effect peaks in this region are sensitive to the solvent polarity and shift to the red by decreasing solvent polarity from methanol to acetonitrile, and then to methylcyclohexane, indicating that the transition involves some n- π^* nature. The theoretical configuration analysis also supported this implication (vide infra). The bands at wavelengths shorter than 260 nm are composed of several transitions such as benzene- π -pyridine- π^* , pyridine π - π^* , and n- π^* transitions and are much sensitive to the nature of solvent. The positive Cotton effect peak observed at around 250 nm in methylcyclohexane almost disappeared in polar solvents, while the Cotton effect at ca. 230 nm was drastically changed by the solvent used. Indeed, the sign of the Cotton effect in this region was inverted between acetonitrile and methanol. This might be explained by the change in (relative contribution of) preferred conformation with a slight change of the solvent property.

In contrast, the pattern of the Cotton effect (i.e., the positive-positive-negative sequence with decreasing wavelength) is preserved for the CD spectra of cationic species **1-Me⁺** in three different solvents (Figure 1, right). The CD spectra of **1-Me⁺** in methanol and in acetonitrile were almost identical. This result can be explained, at least in part, by the fact that the relative contribution of the minor conformers is rather trivial (vide infra). Due to the limited solubility of **1-Me⁺**, we employed dichloromethane as a low-polarity solvent, which unfortunately did not allow us to measure the spectrum in the high energy region (200–230 nm). Although the two positive and one negative Cotton effect peaks were similarly observed as in polar solvents, the relative intensity between the first and second transitions was significantly different in dichloromethane.

b. Temperature-Dependence. We performed the comparative study on temperature-dependence of the CD spectra of **1** and **1-Me⁺**, in order to investigate the equilibrium and the difference in dynamics of the conformers involved. For a direct compari-

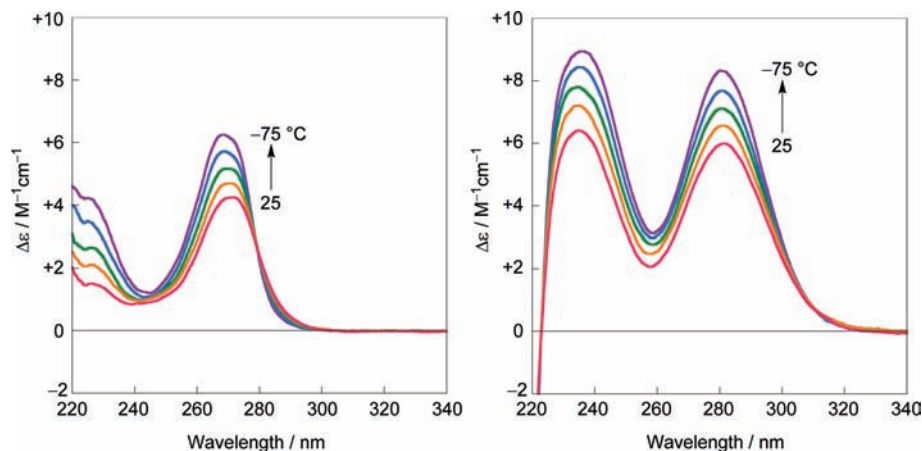


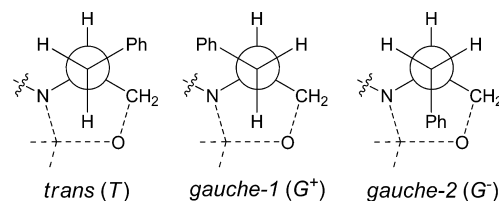
Figure 2. Temperature dependence of the CD spectra of **1** (left) and **1-Me⁺** (right) in methanol. ($T = +25$ to -75 °C at an interval of 25 °C.)

son, we chose methanol as a solvent because of the solubility of both compounds and the relatively wide accessible temperature range of this solvent (Figure 2). As the temperature was lowered, the positive Cotton effects were gradually enhanced for both neutral **1** and cationic **1-Me⁺**. These small changes can be explained by the gradual fixation of the conformation (in addition to the increased concentration by the reduction of the solution volume) at lower temperatures. A close inspection of the temperature-dependence of the CD spectra of neutral **1**, however, revealed a small blue shift of the band at ~ 270 nm upon cooling, while no such shift was observed with cationic **1-Me⁺**. This contrasting behavior implies that a significant shift of the conformational equilibrium is induced by temperature change only for **1**. In cationic **1-Me⁺**, the relative contribution of the predominant conformation does not appear to be changed appreciably in the temperature range examined, probably due to the much stronger cation- π interactions (vide infra). The larger temperature-dependence of the UV-vis spectra of **1**, compared with **1-Me⁺**, is also compatible with this conclusion (Figure S1 in SI).

In the following section, the quantum chemical calculations were performed to obtain further insights into the behavior of the experimental CD spectra of neutral **1** and cationic **1-Me⁺**.

Theoretically Optimized Structures of Nicotinamide 1 and Its Cation- π Derivatives 1-Me⁺ and 2-Me⁺. *a. Geometry Consideration.* For a direct comparison of the observed CD (and absorption) spectra with the theoretical ones for flexible systems, the calculated spectra of all possible conformations should be averaged by taking into account the relative population under the conditions employed. The Boltzmann population-weighted averaging of the spectra calculated for the relevant conformers in local minima (without considering the dynamic behavior) is usually employed as a first approximation to afford the theoretical spectrum that reasonably reproduces the experimental one.⁴ Hence, we first performed the geometry optimization of all possible conformations of **1**, **1-Me⁺**, and **2-Me⁺**. For these species, four conformational freedoms are available: (1) *s-cis/s-trans* conformations around the *C*(pyridine)-*C*(carbonyl) bond, which switches the open face of the benzene ring, (2) rotation around the *C*(benzyl)-*C*(oxazolidine) bond associated with the *trans* and a pair of *gauche* conformers (denoted as *T*, *G⁺*, and *G⁻*; see Chart 2), (3) *syn/anti* conformations around the amide bond, and (4) rotation of the phenyl moiety (for the details of conformational considerations, see text in SI and Chart S1). All of these 36 ($= 2 \times 3 \times 2 \times 3$) conformers were considered initially and fully optimized by the dispersion-corrected DFT-D method. The DFT-D method was selected in

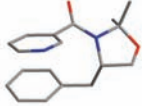
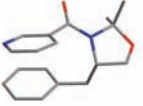
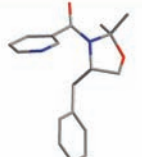
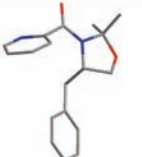
CHART 2: Newman Projections of Trans and Gauche Conformations of Nicotinamide Derivatives 1, 1-Me⁺, and 2-Me⁺ with Respect to the C(benzyl)-C(oxazolidine) Bond

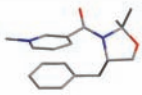
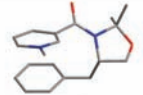


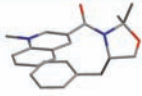
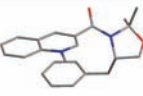
order to effectively describe the weak interactions between the phenyl and the pyridine (or pyridinium) rings.³⁶ Table 1 lists the selected conformers that were considered energetically important for the spectral prediction. We ignored the minor conformations with the energies (ΔE) > 3 kcal mol⁻¹ relative to the most stable conformer, and this procedure left only 4 conformations (pairs of stacked and extended conformers, i.e., *s-trans-G⁺*, *s-cis-G⁺*, *s-trans-T*, and *s-cis-T*) for neutral **1**. For cationic species (**1-Me⁺** and **2-Me⁺**), in contrast, a pair of stacked conformations survived for further spectral study; two extended (*T*) conformations found in neutral **1** became energetically less favorable in cationic forms ($\Delta E > 7$ kcal mol⁻¹, see Tables S1-S3 in SI) due to the lack of effective cation- π interactions in the extended conformations. To obtain the final theoretical spectra, the calculated spectra of conformers were weighted-averaged for the Boltzmann population using the more accurate SCS-MP2 energies (vide infra). The final spectra thus obtained nicely agreed with the experimental ones, validating the above assumption (to ignore the minor conformers of $\Delta E > 3$ kcal mol⁻¹) and the use of cost-efficient contraction for a theoretical CD estimation.

b. Relative Energies. The DFT-D optimized structures obtained in Table 1 were subjected to single-point energy calculation at the SCS-MP2/TZVPP level. The SCS-MP2 is an improved MP2 method, and affords energies comparable to those obtained by the highly costly, but most accurate, CCSD(T) method.²⁶ The energies obtained by the standard DFT and MP2 methods are also included for a comparison purpose (Table 1). For neutral species **1**, the SCS-MP2 and the DFT-D methods gave the comparable relative energies and the agreement between these two methods justifies the applicability of the DFT-D method for the geometry optimization of the present system. This demonstrates the excellent performance of the practically feasible (and thus less-expensive) DFT-D method for geometrical optimizations and also emphasizes the need of van der Waals and/or charge transfer corrections, which are

TABLE 1: Summary of the Geometry Optimization^c

Conformation of 1				
				
ΔE (Population) ^a	<i>s-trans-G</i> ⁺	<i>s-cis-G</i> ⁺	<i>s-trans-T</i>	<i>s-cis-T</i>
DFT-B-LYP/TZV2P	3.67 (1.6%)	4.47 (0.7%)	≡0 (62.4%)	0.57 (35.3%)
DFT-D-B-LYP/TZV2P	≡0 (49.7%)	0.77 (23.0%)	1.13 (16.1%)	1.49 (11.2%)
MP2/TZVPP	≡0 (63.6%)	0.76 (29.7%)	2.77 (4.0%)	3.15 (2.7%)
SCS-MP2/TZVPP	≡0 (53.4%)	0.74 (25.5%)	1.44 (12.7%)	1.85 (8.4%)
SCS-MP2/TZVPP (PCM) ^b	≡0 (40.5%)	0.26 (31.1%)	0.46 (18.8%)	1.44 (9.6%)

Conformation of 1-Me ⁺		
		
ΔE (Population) ^a	<i>s-cis-G</i> ⁺	<i>s-trans-G</i> ⁺
DFT-B-LYP/TZV2P	≡0 (84.8%)	1.72 (15.2%)
DFT-D-B-LYP/TZV2P	≡0 (92.7%)	2.54 (7.3%)
MP2/TZVPP	≡0 (93.9%)	2.73 (6.1%)
SCS-MP2/TZVPP	≡0 (92.5%)	2.51 (7.5%)
SCS-MP2/TZVPP (PCM) ^b	≡0 (75.7%)	1.14 (24.3%)

Conformation of 2-Me ⁺		
		
ΔE (Population) ^a	<i>s-cis-G</i> ⁺	<i>s-trans-G</i> ⁺
DFT-B-LYP/TZV2P	≡0 (93.8%)	2.71 (6.2%)
DFT-D-B-LYP/TZV2P	≡0 (95.2%)	2.99 (4.8%)
MP2/TZVPP	≡0 (94.9%)	2.92 (5.1%)
SCS-MP2/TZVPP	≡0 (95.1%)	2.96 (4.9%)

^a Relative energies in kcal mol⁻¹, calculated for the DFT-D-B-LYP/TZV2P optimized geometries. Populations in parentheses were calculated by applying the Boltzmann population at 25 °C. ^b The PCM model (COSMO; acetonitrile, $\epsilon = 36.64$) was used. ^c The relative energies and isomer populations of neutral nicotinamide **1** and related cation- π derivatives **1-Me**⁺ and **2-Me**⁺ calculated by the standard DFT, DFT-D, MP2, and SCS-MP2 methods.

completely missing in the standard DFT method. Accordingly, both the SCS-MP2 and the DFT-D methods predict the *s-trans-G*⁺ isomer as the most stable conformer with ca. 50% Boltzmann population at 25 °C. The preference for the *s-trans-G*⁺ over the *s-cis-G*⁺ conformer can be explained by an effective cancellation of the dipole moment between the pyridine (or pyridinium) and amide groups in the former conformer (Figure S11 in SI). The MP2 method overestimates the aromatic interaction, as anticipated, predicting slightly higher preference for the folded (*G*⁺) isomers over the extended (*T*) isomers. The standard DFT method, on the contrary, led to a completely different result (predicting *s-trans-T* isomer as the most important conformer). Such a defect in the standard DFT method has been already reported and attributed to a basis set superposition error competing with the errors in intramolecular dispersion.³⁷ Note that the *s-cis-T* isomer was found in the X-ray crystallographic structure,⁶ indicating that a variety of conformers are in the equilibrium in solution. When the simple solvation model (COSMO method)²⁸ was applied to the energy calculation, the extended (*T*) isomers are slightly favored but the effect was essentially negligible. The relative populations calculated by using the SCS-MP2 energies (in the gas phase) are used for obtaining the weighted-averaged theoretical CD spectra throughout the text, since this is more reliable than the other three

methods, and a comparison with the experimental CD spectra shows better reproducibility of the relative excitation energies and rotatory strengths (see Figure S8 in SI). A similar trend (to afford different conformational preference, depending on the calculation method) was also observed for cationic compounds **1-Me**⁺ and **2-Me**⁺, but the effects were less obvious due to the stronger cation- π interaction. The standard DFT method slightly prefers the *s-trans-G*⁺ isomer over the *s-cis-G*⁺ isomer. It is also to note that the minor *s-trans-G*⁺ conformation was found in the X-ray crystallographic structure.⁶

Quantum Chemical Studies of CD Spectra of Nicotinamide 1. a. CD Spectra of 1 in Solution. The experimental CD spectrum of **1** in methylcyclohexane was compared with the theoretical spectra in Figure 3 (left). In our previous studies on the chiral molecules of point, axial, and facial chirality, theoretical CD spectra calculated by the TD-DFT method at the TD-DFT-BH-LYP/TZV2P level successfully reproduced the experimental CD spectra.⁴ Therefore, the CD spectra of **1** were theoretically investigated at the same level. The individual CD spectrum of each conformer differs substantially from the experimental spectrum in sign and intensity. This allows us to critically compare the experimental versus theoretical CD spectra to elucidate the contribution of each conformation in solution (see Figure S5 in SI). The spectra calculated for individual

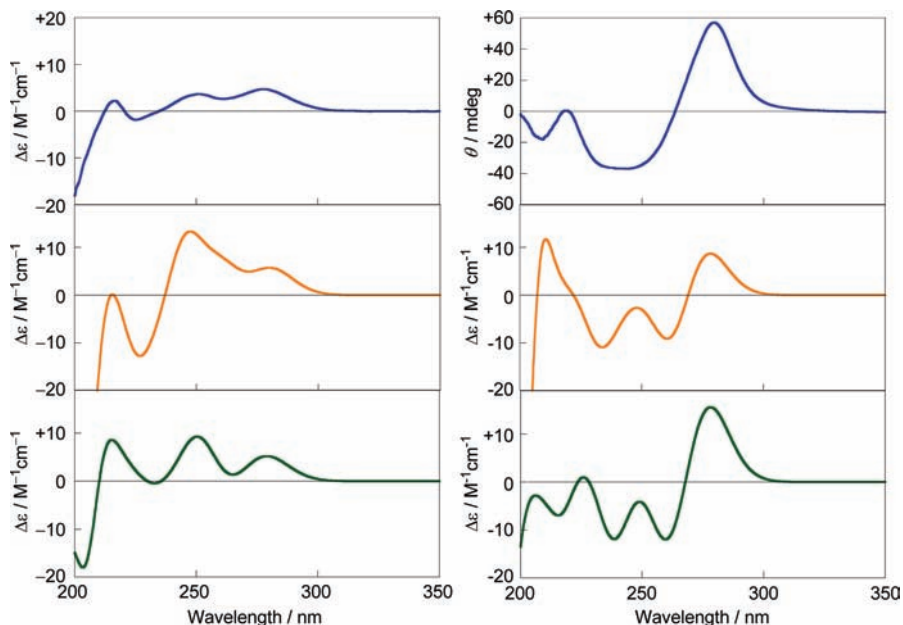


Figure 3. Comparison of experimental CD spectra of **1** in solution and in solid state. Left: Experimental CD spectrum of **1** in methylcyclohexane (top) compared with the theoretical spectra calculated by weighted-averaging all of the reasonably populated conformers at the TD-DFT-BH-LYP/TZV2P level (0.7 eV red shift, 1/2 scaled) (middle) and at the RI-CC2/TZVPP level (0.2 eV red shift and averaged for all conformers) (bottom). Right: Experimental CD spectrum of **1** in KBr (top) compared with the theoretical spectra calculated at the TD-DFT/TZV2P level (middle) and at the RI-CC2/TZVPP level (bottom) for the *s-cis-T* conformation (0.3 eV red shift).

conformers were weighted by the Boltzmann population calculated from the relative SCS-MP2 energies. The averaged CD spectrum of **1** thus obtained was in good agreement with the experimental one in solution. Due to the known deficiency in the TD-DFT method,³⁸ the theoretical spectra were also evaluated with the more accurate time-dependent coupled-cluster calculations that include single and double excitations (albeit with an approximate treatment of the doubles, CC2)³⁹ at the RI-CC2/TZVPP level.

The two positive Cotton effects in the long wavelength region were successfully reproduced by the both methods, but the relative rotatory strengths were better reproduced by the RI-CC2 method. The excitation energies were also better reproduced by the RI-CC2 method, as judged from the applied shift values (0.7 eV for TD-DFT against 0.2 eV for RI-CC2). The pattern followed by these two Cotton effects (i.e., the negative–positive–negative sequence) was qualitatively reproduced by both of the methods, with slight deviation of the relative strengths. It is noteworthy that such spectra can be obtained only by averaging the spectra of 4 conformations; none of the single theoretical CD spectrum agreed with the experimental one. The nice overall agreement of the experimental spectrum in solution with the averaged theoretical spectrum clearly demonstrates that all 4 conformers are appreciably populated (and in equilibrium) in solution, which is in sharp contrast to the result obtained by the X-ray crystallography, where the *s-cis-T* isomer is the sole conformer. The folded (*s-trans-G*⁺ and *s-cis-G*⁺) conformers play considerably important contribution in addition to the extended (*s-trans-T* and *s-cis-T*) conformers in nonpolar methylcyclohexane, probably due to the effective dispersion (London) forces working between the benzene and pyridine rings.⁴⁰ Although the X-ray crystallographic structure is often taken as a solid basis for structure considerations, it is to emphasize that only the comparative experimental and theoretical studies of the CD spectra using a combined state-of-the-art quantum chemical calculations (DFT-D, SCS-MP2, and TD-DFT/RI-CC2 methods) can reveal the

considerable contribution of the seemingly implausible folded conformers in solution.

b. CD Spectra of 1 in Solid Phase. In view of the dramatic change of the preferred conformation, the CD spectrum of neutral **1** in the solid state should be quite different from that in solution. Therefore, we measured the solid-state CD spectrum of **1** in KBr, which was compared with the theoretical spectrum calculated for the conformer found in the X-ray analysis (Figure 3, right). The CD spectrum in the solid state turned out to be quite different from that in solution. Remarkably, the experimental CD spectrum in KBr was again well reproduced by the theory, both in relative excitation energy and rotatory strength. The first largest positive Cotton effect was properly reproduced by both of the theories. The second negative Cotton effect was broad in the experimental spectrum, but was split to give the two distinguished negative peaks in the theoretical one. The spectral reproducibility was better with the RI-CC2 method than with the TD-DFT method, but both methods gave acceptable agreement. The CD spectral measurements in KBr were performed with common precautions to minimize the effects of linear birefringence and linear dichroism (by finely grinding the sample with KBr and measuring the spectra at different angles and faces of the disk). The experimental solid-state CD spectrum of **1** thus obtained nicely agreed with the theoretical one calculated for the *s-cis-T* isomer of **1**, indicating that such artifacts were either negligible or canceled out. Accordingly, one can safely conclude that the *s-cis-T* conformer is preferred in the crystal, while this conformer is less favored in solution; the folded (*s-trans-G*⁺ and *s-cis-G*⁺) conformers are preferred in less polar solvent, but all four conformations are indispensable. The *s-cis-T* conformation favored in the crystal, but less populated in solution, may be explained by the packing forces in the crystal lattice.

Theoretical CD Spectra of Cation- π Species. a. Theoretical CD Spectra of 1-Me⁺. The experimental CD spectrum of **1-Me**⁺ as a bromide salt was obtained only in dichloromethane and more polar solvents, due to the low solubility

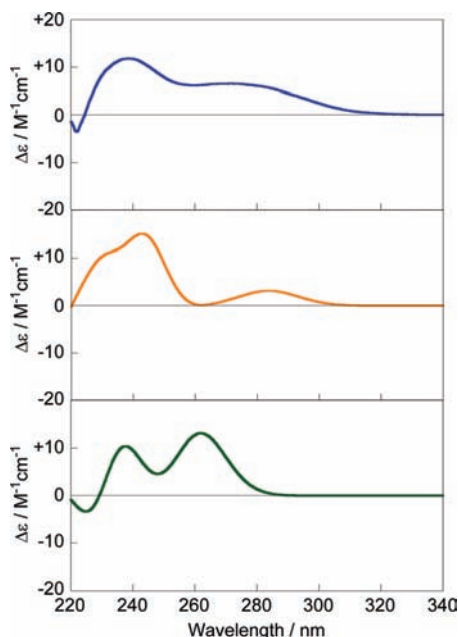


Figure 4. Comparison of the experimental CD spectrum of **1-Me**⁺ in dichloromethane (top) with the calculated spectra at the TD-DFT-BH-LYP/TZV2P level (0.3 eV blue shift, 1/2 scaled) (middle), and at the RI-CC2/TZVPP level (1.0 eV blue shift, conformer-distribution averaged) (bottom).

of this pyridinium salt in less polar solvents. The experimental spectrum in dichloromethane was compared with the theoretical spectra calculated at the TD-DFT-BH-LYP/TZV2P and the RI-CC2/TZVPP levels (Figure 4, middle and bottom, respectively). The two positive Cotton effects observed at around 240 and 270 nm were properly reproduced by the theory, and the TD-DFT method afforded slightly better (apparent) agreement with the experiment. The well-known underestimation of the charge-transfer transition by the TD-DFT method was also noticeable and thus the calculated spectrum was blue-shifted by 0.3 eV. In the RI-CC2 calculation, the transition energies of two positive Cotton effects and higher-energy transitions were totally underestimated. The poorer reproduction of the spectra of **1-Me**⁺, even with the more accurate RI-CC2 method, remains to be rationalized, but may be attributable in part to the complete ignorance of the solvent effect in our calculation. The experimental CD spectrum of **1-Me**⁺ was highly dependent on the solvent polarity (vide supra). Indeed, the calculated spectrum better agreed with the experimental spectrum in acetonitrile or methanol, thus implying the lack of proper description of solvent effect. Use of the COSMO method in energy calculations was not helpful in improving the theoretical CD spectra. Probably, more specific interactions between the cationic moiety and solvent molecules are involved, which cannot be described by such a PCM model.⁴¹

Although these theoretical spectra were produced by averaging the two conformers weighted by the Boltzmann population, the spectra profoundly reflect the nature of the *s-cis-G*⁺ conformation due to the population of up to 92%. The agreement of these spectra with the experimental one clearly indicates the importance of the *s-cis-G*⁺ conformer in solution. The *s-trans-G*⁺ isomer, found in the crystal structure, exhibits a quite different CD spectral pattern, and cannot be the major conformer in solution. This conclusion is also supported by the stereoselectivity found in the nucleophilic reaction,⁶ in which the nucleophiles attack from the open B-side, while the A-side is stacked in the *s-cis-G*⁺ conformation.

b. Configuration Analysis of the Transitions of **1-Me**⁺.

Although the CD spectrum of neutral **1** is a weighted average of completely different spectra of four independent conformers, the CD spectrum of **1-Me**⁺ can be described essentially by a single species (Table 1). Thus, we analyzed the nature and configuration of the transitions of cationic **1-Me**⁺ from the theoretical calculation of the *s-cis-G*⁺ conformer of **1-Me**⁺ (Tables 2 and 3). [A similar analysis was also performed for the most abundant conformer of neutral **1** (Tables S5–S6 in SI)]. A close comparison of the experimental spectrum with the theoretical one calculated by the RI-CC2 method reveals that the first and second transitions observed in the experimental spectrum consist of a pair of transitions. Therefore, the first positive, second positive, and third negative Cotton effects were nicely reproduced by this method, with a slight underestimation (0.8–1.0 eV) of the transition energies. The first band is assignable to a mixture of transitions that mostly come from the *n-π** and (pyridinium) *π-π**. The second band contains some charge-transfer transitions together with the *π-π** transition. Note that the complete assignment is not very straightforward due to a mixing of several transitions (Table 3 and Figure 5). Since the apparently coupled CD signals in the experimental spectrum are not of the same origin, the empirical exciton chirality rule should not be applied; a close examination of the configuration revealed that such an exciton coupling interaction is unfeasible for most of the major transitions. Configuration analysis for the results from the TD-DFT method revealed that the agreement of the experimental and theoretical spectra was a mere coincidence, probably by an error cancellation. In addition, a number of so-called ghost peaks were observed. Although the TD-DFT seems to be a sensible method for balancing efficiency (low computation times) with reliability, it tends to exhibit certain flaws in such systems that contain ionic, charge-transfer, Rydberg, and multiple-excitation characters.⁴²

c. Theoretical CD Spectra of **2-Me⁺.** In order to further investigate the effect of intramolecular electronic interaction between the cationic moiety with the benzene ring on the CD spectrum, we then employed the quinolinium derivative **2-Me**⁺. Because the transitions of benzene and pyridinium are significantly overlapped with each other in **1-Me**⁺, changing the pyridinium to a quinolinium will lead to more discrete transitions, affording additional information concerning the nature of transitions. Due to the relatively large number of atoms involved, the RI-CC2 calculation, which is formally scaled to *N*⁵ (*N*: number of orbitals),³¹ was not practically accessible for **2-Me**⁺ (see Table S4 in SI for a detail). Thus, the result from the TD-DFT method was compared with the experimental spectrum in acetonitrile (Figure 6). The theoretical spectrum was obtained by averaging the spectra of two conformers using the SCS-MP2 energies as treated previously. Although there are some deviations in Cotton effects, the first positive, second positive, third positive (and as twice as large in strength), and fourth negative Cotton effects are properly reproduced. The deviations are found mostly at the ¹*L*_a and ¹*L*_b transitions of quinolinium, which is however a known deficiency in the TD-DFT method. The substantial errors in the ¹*L*_a and ¹*L*_b transitions of naphthalene and related systems have been already reported for the current density functional.⁴³

The overall agreement of the theoretical spectrum with the experimental one supports the conclusion that in solution the folded *s-cis-G*⁺ conformer is much favored over the extended *s-trans-G*⁺ isomer for both **1-Me**⁺ and **2-Me**⁺. Therefore, with a proper choice of the functional and an appropriate basis-set,

TABLE 2: Comparison of Experimental and Calculated Excited-State Properties of Most Stable *s-cis-G*⁺ Conformer of Cationic 1-Me⁺^a

	transition energy			rotatory strength			oscillator strength		
	exp.	RI-CC2	TD-DFT	exp.	RI-CC2	TD-DFT	exp.	RI-CC2	TD-DFT
first	4.51	3.68	4.06	+0.027	+0.009	+0.0143	0.010	0.008	0.003
second		3.74	4.33		+0.052	+0.0019		0.050	0.004
third	5.21	4.27	4.61	+0.048	+0.008	-0.0098	0.011	0.001	0.006
fourth		4.28	4.78		+0.057	+0.0649		0.009	0.063
fifth	5.29	4.40	4.89	-0.038	-0.038	-0.0146	0.024	0.028	0.028

^a The first two transitions in the experimental spectra consist of a pair of transitions in the RI-CC2 calculations. Transition energies are reported in eV and the rotatory and oscillator strengths are in atomic unit.

TABLE 3: Comparison of RI-CC2 and TD-DFT-BH-LYP Configuration Analysis for Major Transitions of the *s-cis-G*⁺ Conformer of 1-Me⁺^a

	RI-CC2		TD-DFT	
first	HOMO-2 \rightarrow LUMO ($n-\pi^*$)	(62%)	HOMO \rightarrow LUMO (CT)	(98%)
	HOMO \rightarrow LUMO (CT)	(13%)		
	HOMO-3 \rightarrow LUMO ($n-\pi^*$)	(10%)		
second	HOMO-5 \rightarrow LUMO (pyridinium $\pi-\pi^*$)	(37%)	HOMO-1 \rightarrow LUMO (CT)	(98%)
	HOMO-3 \rightarrow LUMO ($n-\pi^*$)	(25%)		
	HOMO-2 \rightarrow LUMO ($n-\pi^*$)	(19%)		
third	HOMO \rightarrow LUMO (CT)	(65%)	HOMO-2 \rightarrow LUMO ($n-\pi^*$)	(90%)
	HOMO-2 \rightarrow LUMO ($n-\pi^*$)	(18%)		
fourth	HOMO-5 \rightarrow LUMO+1 (pyridinium $\pi-\pi^*$)	(45%)	HOMO-4 \rightarrow LUMO ($n-\pi^*$)	(73%)
	HOMO-3 \rightarrow LUMO+1 ($n-\pi^*$)	(25%)		
fifth	HOMO-2 \rightarrow LUMO+1 ($n-\pi^*$)	(75%)	HOMO \rightarrow LUMO+1 (CT)	(94%)
	HOMO \rightarrow LUMO+1 (CT)	(16%)		

^a Molecular orbitals and their classification of all major contributions ($\geq 10\%$) in the first 5 transitions were selected. Relative contributions are in parentheses.

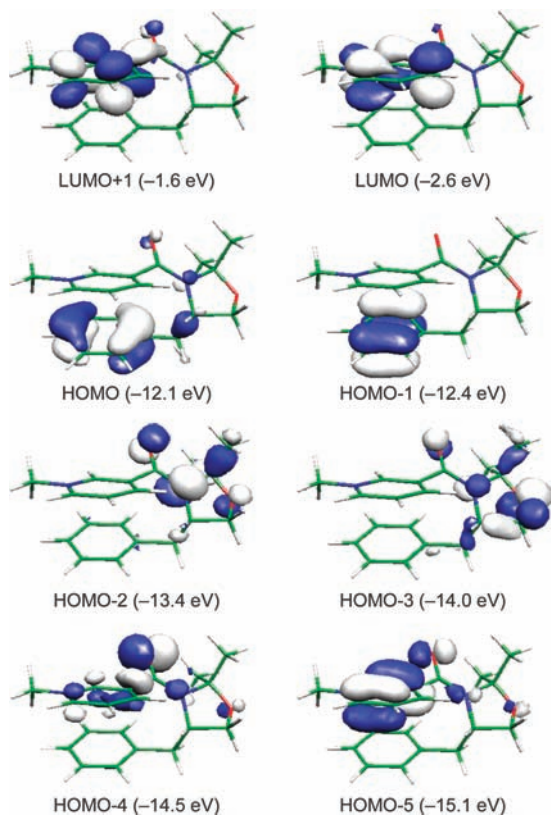


Figure 5. Relevant molecular orbitals of most abundant *s-cis-G*⁺ conformer of 1-Me⁺ involved in the first 5 transitions at the RI-CC2/TZVPP level.

the TD-DFT method is able to provide solid information concerning the structural (conformational) behavior in solution, when combined with the experimental CD spectral investigation.

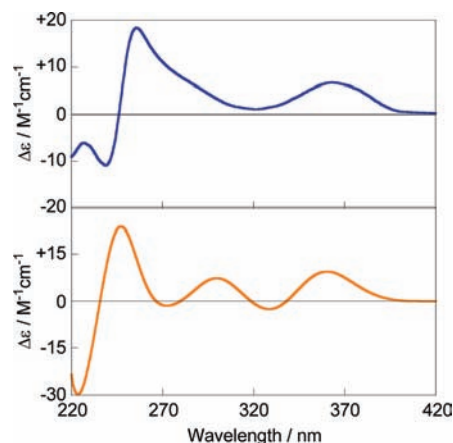


Figure 6. Comparison of experimental CD spectra of 2-Me⁺ (top) with the calculated one at the TD-DFT/TZV2P level (0.3 eV blue shift). The spectrum was obtained by averaging two conformations.

Theoretical Studies of the Optical Rotations. The comparison of experimental and calculated specific rotations, in addition to the above chiroptical analyses of the CD spectra, would reinforce the elucidation of structural variation of nicotinamides **1** and its cation- π derivatives in solution. It is to note however that the costs of calculations are almost parallel (or slightly higher as the diffuse functions are necessary) for the specific rotations and the CD spectra. Table 4 summarizes the experimental and theoretical specific rotations for **1**, 1-Me⁺, and 2-Me⁺. Although the specific rotation of **1** in chloroform has been reported, we measured the value in nonpolar methylcyclohexane. The value was slightly solvent dependent but varied only in a range of 11–13°. The calculation of specific rotation by the TD-DFT-BH-LYP method for the relevant conformers of **1** revealed that the folded (*G*⁺) conformers afford positive rotations, while the extended (*T*) conformers afford

TABLE 4: Summary of the Experimental and Theoretical Specific Rotations ($[\alpha]_D$) for **1, **1-Me⁺**, and **2-Me⁺**^a**

compound/conformer	experimental $[\alpha]_D$	theoretical $[\alpha]_D$		
		aug-SVP	aug-cc-pVDZ ^f	aug-cc-pVTZ
1	+11.1 (<i>c</i> 1.0, CHCl ₃) ^b +13.0 (<i>c</i> 1.5, MCH) ^c	+272 ^e	+153 (+465) ^e	+159
<i>s-trans-G⁺</i>		+383	+310 (+641)	+299
<i>s-cis-G⁺</i>		+374	+227 (+628)	+204
<i>s-trans-T</i>		-218	-290 (-274)	-295
<i>s-cis-T</i>		-0	-168 (-32)	-184
1-Me⁺	+97.1 (<i>c</i> 1.4, CH ₂ Cl ₂) ^c	+665 ^e	+530 (+1693) ^e	+510
<i>s-cis-G⁺</i>		+653	+518 (+1725)	+496
<i>s-trans-G⁺</i>		+715	+688 (+1304)	+677
2-Me⁺	+137.7 (<i>c</i> 1.1, CH ₃ CN) ^d	+1100 ^e	+859 (+3025) ^e	+851
<i>s-cis-G⁺</i>		+1170	+943 (+3192)	+910
<i>s-trans-G⁺</i>		-77	-251 (-223)	-267

^a Experimental specific rotation at the sodium-D line ($[\alpha]_D$) at 20–24 °C. The theoretical specific rotations were calculated by the TD-DFT-BH-LYP method with the basis-set indicated. ^b From ref 44. ^c This work; MCH = methylcyclohexane. ^d From ref 35. ^e The values were averaged by the Boltzmann population based on the SCS-MP2 energies. ^f The B3-LYP functional was used for values in parentheses.

negative ones. Averaging these values by using the Boltzmann population based on the SCS-MP2 energies (Table 1) successfully reproduced the positive sign of the experimental specific rotation. This result confirms the previous conclusion that the extended conformers are not the major conformers in solution (vide supra). However the computed absolute value was much larger. Such discrepancy may be tracked back to the ignorance of the dynamic behavior in our calculation, or by the deficiencies of the current TD-DFT method. Similarly, the theoretical specific rotations calculated for **1-Me⁺** or **2-Me⁺** gave the correct signs, but were less informative than the CD spectra.

Summary and Conclusions

Molecular structure (conformation) is a critical function of the surroundings or the conditions employed. It is often the case therefore that the solution-phase structure under the actual reaction condition is significantly different from the X-ray crystallographic structure. Thus, the crystal structure is an excellent source of the physical parameters of molecules such as bond length, dihedral angle, etc. but is not suitable for discussing the possible conformations in solution and sometimes misleads to an erroneous reaction mechanism or (stereo)selectivity prediction. Furthermore, in discussion based on the crystal structure, the equilibrium and dynamics of conformers are not considered in general, despite their potential roles in the overall reaction mechanisms.

In this work to investigate the solution-phase conformations of neutral and cationic (*N*-methylated) nicotinamide derivatives with and without cation- π interactions, we have demonstrated that the combined experimental and theoretical studies of chiroptical properties serve as a powerful standard tool for elucidating the structures and relative energies of possible conformers in solution. The major findings, recommendations, and conclusions are summarized as follows:

1. Experimental CD Spectra. As the calculations give the gas-phase structures in general, the use of less- to nonpolar solvents is highly recommended in experimental CD measurement for a comparison with the theoretical ones. The temperature and solvent effects on the experimental CD spectra of **1**, **1-Me⁺**, and **2-Me⁺** afforded the additional information about the conformer equilibrium and population in solution. The CD spectrum of **1** in the solid state provided the complementary information for one of the conformers that exist in solution.

2. Geometry Optimizations. The dispersion-corrected DFT calculation (DFT-D) at the B-LYP/TZV2P level of nicotinamide **1** revealed that the pairs of stacked and extended conformers,

i.e., *s-trans-G⁺*, *s-cis-G⁺*, *s-trans-T*, and *s-cis-T*, are populated. For the cation- π derivatives, only the two folded conformers were shown to be essential.

3. Relative Contribution of the Conformers. Energy calculation by the SCS-MP2 method with the TZVPP basis-set, used for the nicotinamides to obtain the final Boltzmann population of the conformers, was shown to be very reliable. The DFT-D/TZV2P energies were similar to the SCS-MP2 energies, which also justifies the use of cost-efficient DFT-D method for geometry optimization. The standard DFT method failed to predict the correct relative energies (and ordering) in **1**, as was sometimes pointed out in cases where the vdW and/or CT interactions are important.

4. Time Dependent DFT and CC2 Calculations. Since the two chromophores in the present systems are closely located and considerably interacting, the inclusion of the excited doubles in the RI-CC2 calculation led to the better reproducibility of the observed spectra. Boltzmann averaging of all relevant conformers by using the SCS-MP2 relative energies nicely reproduced the experimental spectrum of neutral **1**, confirming the existence and relative contribution of each calculated conformer. The same method applied to the prediction of the spectrum of **1** in the solid state also gave a good agreement with the experimental one. The theoretical spectra of cation- π derivatives **1-Me⁺** and **2-Me⁺** agreed with the experimental ones less satisfactorily. Nevertheless, the major contribution of the solid-state conformer (*s-trans-G⁺*) in solution phase can be readily excluded. Although the cation- π interactions are valid both in solution and in crystals, the face-flipped conformer (*s-cis-G⁺*) becomes the major conformer in solution for both **1-Me⁺** and **2-Me⁺**.

5. Configuration Analysis. Since the chromophores are closely located and interacting with each other in the cation- π species, the bands are composed of a complicated mixture of transitions and therefore the correct assignment of the CD spectra became feasible only with the more sophisticated methods. The use of empirical exciton coupling theory without knowing the nature of the transitions should be avoided.

6. Optical Rotation. The comparative experimental and theoretical study of optical rotation was less informative than the CD spectral studies, simply affording the matched sign and relative magnitude of the specific rotations for **1**, **1-Me⁺**, and **2-Me⁺**.

From the viewpoint of reaction mechanism, it is interesting to point out that the folded conformations are only feasible for cation- π derivative **1-Me⁺**, but the *s-cis-G⁺* conformer, in

which the stacked benzene face is opposite to that observed in the X-ray structure, is the dominant conformation in solution. The stereoselectivities upon nucleophilic attack reported earlier⁶ can be successfully explained if this is the dominant conformer in solution. Although such inconsistency between the crystal structure and the solution conformations may not always occur, the X-ray structure alone cannot be conclusive or even misleading in discussing the structure and reactivity of the relevant species in solution, especially where the weak interactions, such as vdW, CT, and cation- π interactions, are involved.

We think the present study using a rather challenging cation- π species is an excellent example that demonstrates how the state-of-the-art quantum chemical calculations together with the experimental CD spectra are able to provide detailed insights into the conformer structure, energy, and population in solution. Quantum chemical geometry optimization is nowadays a conventional task, but the theoretical calculation alone predicts a variety of possible structures/conformations and sometimes affords contradictory results depending on the level of calculation employed. Therefore a verification of the chosen method (in addition to the justification based on the theoretical background) for geometry optimization should be carried out, and further recommendation (for the chiral molecules) is a combined use of experimental/theoretical CD spectral methods, which enables quasi-quantitative discussion of the structures and the relative contribution of the conformers in solution.

Acknowledgment. T.M. thanks the Alexander von Humboldt-Stiftung for the fellowship. Financial supports of this work by a Grant-in-Aid for Scientific Research in a Priority Area "New Frontiers in Photochromism (No. 471)" and a Grant-in-Aid for Scientific Research (No. 21750044) from the Ministry of Education, Culture, Sports, Science and Technology (MEXT), Japan and by Mitsubishi Chemical Corporation Fund (to T.M.) are gratefully acknowledged. Y.I. thanks the support of this work by a Grant-in-Aid for Scientific Research (A) from JSPS (No. 21245011).

Supporting Information Available: Details of geometry considerations and summary of optimization, theoretical and experimental UV-vis and CD spectra under a variety of conditions, theoretical CD spectra of each conformer, configuration analysis and molecular orbitals of most abundant conformer of **1**, and Cartesian coordinates of the optimized geometries of a variety of conformations of **1**, **1-Me⁺**, and **2-Me⁺**. This material is available free of charge via the Internet at <http://pubs.acs.org>.

References and Notes

- (1) (a) *Time-Dependent Density Functional Theory*; Marques, M. A. L., Ullrich, C. A., Nogueira, F., Rubio, A., Burke, K., Gross, E. K. U., Eds.; Springer-Verlag: Berlin-Heidelberg, Germany, 2006. (b) Casida, M. E. *Time-Dependent Density Functional Response Theory for Molecules*. In *Recent Advances in Density Functional Methods*; Chong, D. P., Ed.; World Scientific: Singapore, 1995; Vol. 1, pp 155–192.
- (2) (a) Gangemi, F.; Gangemi, R.; Longhi, G.; Abbate, S. *Phys. Chem. Chem. Phys.* **2009**, *11*, 2683–2689. (b) Timothy, F.; Rudd, R.; Nichols, R. J.; Yates, E. A. *J. Am. Chem. Soc.* **2008**, *130*, 2138–2139. (c) Izumi, H.; Ogata, A.; Nafie, L. A.; Dukor, R. K. *J. Org. Chem.* **2008**, *73*, 2367–2372. (d) Izumi, H.; Futamura, S.; Tokita, N.; Hamada, Y. *J. Org. Chem.* **2007**, *72*, 277–279. (e) Monde, K.; Miura, N.; Hashimoto, M.; Taniguchi, T.; Inabe, T. *J. Am. Chem. Soc.* **2006**, *128*, 6000–6001. (f) Mori, T.; Izumi, H.; Inoue, Y. *J. Phys. Chem. A* **2004**, *108*, 9540–9549. In contrast, signals are rather superabundant in most of the VCD studies, which prevents detailed analysis. See for example: Devlin, J.; Stephens, P. J. *J. Org. Chem.* **2005**, *70*, 2980–299.
- (3) (a) Hembury, G. A.; Borovkov, V. V.; Inoue, Y. *Chem. Rev.* **2008**, *108*, 1–73. (b) Berova, N.; Nakanishi, K.; Woody, R. W. *Circular Dichroism: Principles and Applications*, 2nd ed.; Wiley: New York, 2000.
- (4) (a) Mori, T.; Inoue, Y.; Grimme, S. *J. Org. Chem.* **2006**, *71*, 9797–9806. (b) Mori, T.; Inoue, Y.; Grimme, S. *J. Phys. Chem. A* **2007**, *111*, 7995–8006. (c) Mori, T.; Inoue, Y.; Grimme, S. *J. Phys. Chem. A* **2007**, *111*, 4222–4234. (d) Fukui, M.; Mori, T.; Inoue, Y.; Rajendra, R. *Org. Lett.* **2007**, *9*, 3977–3980.
- (5) (a) Bringmann, G.; Gulder, T. A. M.; Reichert, M.; Gulder, T. *Chirality* **2008**, *20*, 628–642. (b) Honda, Y.; Kurihara, A.; Hada, M.; Nakatsuji, H. *J. Comput. Chem.* **2008**, *29*, 612–621. (c) Grkovic, T.; Ding, Y.; Li, X. C.; Webb, V. L.; Ferreira, D.; Copp, B. R. *J. Org. Chem.* **2008**, *73*, 9133–9136. (d) Fan, J.; Seth, M.; Autschbach, J.; Ziegler, T. *Inorg. Chem.* **2008**, *47*, 11656–11668. (e) Giorgio, E.; Tanaka, K.; Verotta, L.; Nakanishi, K.; Berova, N.; Rosini, C. *Chirality* **2007**, *19*, 434–445. (f) Ding, Y.; Li, X. C.; Ferreira, D. *J. Org. Chem.* **2007**, *72*, 9010–9017.
- (6) Yamada, S.; Morita, C. *J. Am. Chem. Soc.* **2002**, *124*, 8184–8185.
- (7) For a review, see: Ma, J. C.; Dougherty, D. A. *Chem. Rev.* **1997**, *97*, 1303–1324. See also: Dougherty, D. A. *Science* **1996**, *271*, 163–168.
- (8) (a) Burley, S. K.; Petsko, G. A. *FEBS Lett.* **1986**, *203*, 139–143. (b) Singh, J.; Thornton, J. M. *J. Mol. Biol.* **1990**, *211*, 595–615. (c) Meyer, E. A.; Castellano, R. K.; Diederich, F. *Angew. Chem., Int. Ed.* **2003**, *42*, 1210–1250. (d) Matsumura, H.; Yamamoto, T.; Leow, T. C.; Mori, T.; Salleh, A. B.; Basri, M.; Inoue, T.; Kai, Y.; Abd Rahman, R. N. Z. R. *Proteins* **2007**, *70*, 592–598. (e) Zürcher, M.; Diederich, F. *J. Org. Chem.* **2008**, *73*, 4345–4361. (f) Shukla, R.; Lindeman, S. V.; Rathore, R. *J. Am. Chem. Soc.* **2006**, *128*, 5328–5329. (g) Rathore, R.; Chebny, V. J.; Abdelwahed, S. H. *J. Am. Chem. Soc.* **2005**, *127*, 8012–8013. (h) Rathore, R.; Abdelwahed, S. H.; Guzei, I. A. *J. Am. Chem. Soc.* **2004**, *126*, 13582–13583.
- (9) Sunner, J.; Nishizawa, K.; Kebarle, P. *J. Phys. Chem.* **1981**, *85*, 1814–1820.
- (10) For a recent example of investigation of cation- π interaction in brain receptors with nicotine, see: Xiu, X.; Puskar, N. L.; Shanata, J. A. P.; Lester, H. A.; Dougherty, D. A. *Nature* **2009**, *458*, 534–538.
- (11) (a) Wheeler, S. E.; Houk, K. N. *J. Am. Chem. Soc.* **2009**, *131*, 3126–3127. (b) Singh, N. J.; Min, S. K.; Kim, D. Y.; Kim, K. S. *J. Chem. Theory Comput.* **2009**, *5*, 515–529. (c) Wu, R.; McMahon, T. B. *J. Am. Chem. Soc.* **2008**, *130*, 12554–12555.
- (12) For a recent theoretical investigation on the metal cation- π interactions, see: (a) Tsuzuki, S.; Yoshida, M.; Uchimaru, T.; Mikami, M. *J. Phys. Chem.* **2001**, *105*, 769–773. (b) Gallivan, J. P.; Dougherty, D. A. *Proc. Natl. Acad. Sci. U.S.A.* **1999**, *96*, 9459–9464. (c) Cubero, E.; Luque, F. J.; Orozco, M. *Proc. Natl. Acad. Sci. U.S.A.* **1998**, *95*, 5976–5980. (d) Mecozi, S.; West, A. P., Jr.; Dougherty, D. A. *J. Am. Chem. Soc.* **1996**, *118*, 2307–2308.
- (13) (a) Yamada, S.; Yamamoto, J.; Ohta, E. *Tetrahedron Lett.* **2007**, *48*, 855–858. (b) Yamada, S.; Morimoto, Y.; Misono, T. *Tetrahedron Lett.* **2005**, *46*, 5673–5676. (c) Yamada, S.; Misono, T.; Tsuzuki, S. *J. Am. Chem. Soc.* **2004**, *126*, 9862–9872.
- (14) (a) Yamada, S.; Tokugawa, Y. *J. Am. Chem. Soc.* **2009**, *131*, 2098–2099. (b) Yamada, S.; Uematsu, N.; Yamashita, K. *J. Am. Chem. Soc.* **2007**, *129*, 12100–12101.
- (15) (a) Lee, K. Y.; Kochi, J. K. *J. Chem. Soc., Perkin Trans. 2* **1994**, 237–245. (b) Lee, K. Y.; Kochi, J. K. *J. Chem. Soc., Perkin Trans. 2* **1994**, 1011–1017.
- (16) Tsuzuki, S.; Mikami, M.; Yamada, S. *J. Am. Chem. Soc.* **2007**, *129*, 8656–8662.
- (17) (a) Comba, P.; Kerscher, M.; Lampeka, Y. D.; Lotzbeyer, L.; Pritzkow, H.; Tsymbal, L. V. *Inorg. Chem.* **2003**, *42*, 3387–3389. (b) Arunkumar, N.; Ramamurthy, V. *Org. Biomol. Chem.* **2006**, *4*, 4533–4542. (c) Parrish, J. P.; Trzupek, J. D.; Hughes, T. V.; Hwang, I.; Boger, D. L. *Bioorg. Med. Chem.* **2004**, *12*, 5845–5856.
- (18) (a) Rosokha, S. V.; Newton, M. D.; Jalilov, A. S.; Kochi, J. K. *J. Am. Chem. Soc.* **2008**, *130*, 1944–1952. (b) Rosokha, S. V.; Kochi, J. K. *J. Am. Chem. Soc.* **2007**, *129*, 3683–3697. (c) Rosokha, S. V.; Kochi, J. K. *J. Am. Chem. Soc.* **2007**, *129*, 828–838. (d) Rosokha, S. V.; Kochi, J. K. *J. Org. Chem.* **2002**, *67*, 1727–1737.
- (19) (a) Rathore, R.; Hecht, J.; Kochi, J. K. *J. Am. Chem. Soc.* **1998**, *120*, 13278–13279. (b) Brown, R. S.; Nagorski, R. W.; Benuet, A. J.; McClung, R. E. D.; Aarts, J. G. H. M.; Klobukowski, M.; McDonald, R.; Santaniero, B. D. *J. Am. Chem. Soc.* **1994**, *116*, 2448–2456. (c) Mori, T.; Rathore, R.; Lindeman, S. V.; Kochi, J. K. *Chem. Commun.* **1998**, 927–928.
- (20) Bastiaansen, L. A. M.; Vermeulen, T. J. M.; Buck, H. M.; Smeets, W. J. J.; Kanters, J. A.; Spek, A. L. *Chem. Commun.* **1988**, 230–231.
- (21) (a) Richter, I.; Warren, M. R.; Minari, J.; Elfeky, S. A.; Chen, W.; Mahon, M. F.; Raithby, P. R.; James, T. D.; Sakurai, K.; Teat, S. J.; Bull, S. D.; Fossey, J. S. *Chem. Asian J.* **2009**, *4*, 194–198. (b) Richter, I.; Minari, J.; Axe, P.; Lowe, P. J.; James, D. T.; Sakurai, K.; Bull, D. S.; Fossey, S. J. *Chem. Commun.* **2008**, 1082–1084. (c) Comba, P.; Kerscher, M.; Lampeka, Y. D.; Lotzbeyer, L.; Pritzkow, H.; Tsymbal, L. V. *Inorg. Chem.* **2003**, *42*, 3387–3389.
- (22) For recent reviews on ab-initio calculation of chiroptical properties, see: (a) Crawford, T. D. *Theor. Chem. Acc.* **2006**, *115*, 227–245. (b) Crawford, T. D.; Tam, M. C.; Abrams, M. L. *J. Phys. Chem. A* **2007**, *111*,

12057–12068. See also: (c) Diedrich, C.; Grimme, S. *J. Phys. Chem. A* **2003**, *107*, 2524–2539. (d) Goerigk, L.; Grimme, S. *J. Phys. Chem. A* **2009**, *113*, 767–776.

(23) Ahlrichs, R.; Bär, M.; Baron, H. P.; Bauernschmitt, R.; Böcker, S.; Ehrig, M.; Eichkorn, K.; Elliott, S.; Furche, F.; Haase, F.; Häser, M.; Horn, H.; Huber, C.; Huniar, U.; Kattannek, M.; Kölmel, C.; Kollwitz, M.; May, K.; Ochsenfeld, C.; Öhm, H.; Schäfer, A.; Schneider, U.; Treutler, O.; von Arnim, M.; Weigend, F.; Weis, P.; Weiss, H. *TURBOMOLE*, version 5.9; Universität Karlsruhe: Karlsruhe, 2005. See also: http://www.cosmologic.de/QuantumChemistry/main_turbomole.html.

(24) (a) Grimme, S.; Diedrich, C.; Korth, M. *Angew. Chem., Int. Ed.* **2006**, *45*, 625–629. (b) Piacenza, M.; Grimme, S. *J. Am. Chem. Soc.* **2005**, *127*, 14841–14848. (c) Piacenza, M.; Grimme, S. *Chem. Phys. Chem.* **2005**, *6*, 1554–1558. (d) Grimme, S. *J. Comput. Chem.* **2004**, *25*, 1463–1473.

(25) (a) Eichkorn, K.; Treutler, O.; Öhm, H.; Häser, M.; Ahlrichs, R. *Chem. Phys. Lett.* **1995**, *240*, 283–289. (b) Weigend, F.; Häser, M. *Theor. Chem. Acc.* **1997**, *97*, 331–340. (c) Grimme, S.; Waletzke, M. *Phys. Chem. Chem. Phys.* **2000**, *2*, 2075–2081. (d) Vahtras, O.; Almlöf, J.; Feyereisen, M. W. *Chem. Phys. Lett.* **1993**, *213*, 514–518. (e) Hättig, C.; Weigend, F. *J. Chem. Phys.* **2000**, *113*, 5154–5161.

(26) (a) Grimme, S. *J. Phys. Chem. A* **2005**, *109*, 3067–3077. (b) Goumans, T. P. M.; Ehlers, A. W.; Lammertsma, K.; Würthwein, E.-U.; Grimme, S. *Chem.—Eur. J.* **2004**, *10*, 6468–6475. (c) Grimme, S. *J. Chem. Phys.* **2003**, *118*, 9095–9102. (d) Gerenkamp, M.; Grimme, S. *Chem. Phys. Lett.* **2004**, *392*, 229–235. (e) Grimme, S. *J. Comput. Chem.* **2003**, *24*, 1529–1537. (f) Piacenza, M.; Grimme, S. *J. Comput. Chem.* **2004**, *25*, 83–99.

(27) (a) Grimme, S. *Angew. Chem., Int. Ed.* **2006**, *45*, 4460–4464, and references cited therein. (b) Grimme, S.; C. Diedrich, S.; Korth, M. *Angew. Chem., Int. Ed.* **2006**, *45*, 625–629.

(28) (a) Tomasi, J.; Persico, M. *Chem. Rev.* **1994**, *94*, 2027–2094. (b) Sinnecker, S.; Rajendran, A.; Klamt, A.; Diedenhofen, M.; Neese, F. *J. Phys. Chem. A* **2006**, *110*, 2235–2245. See also: (c) Pecul, M.; Marchesan, D.; Ruud, K.; Coriani, S. *J. Chem. Phys.* **2005**, *122*, 024106.

(29) Grimme, S. *Rev. Comput. Chem.* **2004**, *20*, 153–218. (b) Dreuw, A.; Head-Gordon, M. *Chem. Rev.* **2005**, *105*, 4009–4037. (c) Polavarapu, P. L. *Chirality* **2002**, *14*, 768–781.

(30) Notations from Gaussian package corresponds to: BH&HLYP. See also: (a) Maity, D. K.; Duncan, W. T.; Truong, T. N. *J. Phys. Chem. A* **1999**, *103*, 2152–2159. (b) Duncan, W. T.; Truong, T. N. *J. Chem. Phys.* **1995**, *103*, 9642–9652. (c) Liao, M.-S.; Lu, Y.; Scheiner, S. *J. Comput. Chem.* **2003**, *24*, 623–631.

(31) (a) Christiansen, O.; Koch, H.; Jörgensen, P. *Chem. Phys. Lett.* **1995**, *243*, 409–418. (b) Hättig, C.; Köhn, A. *J. Chem. Phys.* **2002**, *117*, 6939–6951.

(32) Bauernschmitt, R.; Ahlrichs, R. *Chem. Phys. Lett.* **1996**, *256*, 454–464.

(33) Hättig, C.; Weigend, F. *J. Chem. Phys.* **2000**, *113*, 5154–5161.

(34) (a) Dunning, T. H. *J. Chem. Phys.* **1993**, *98*, 7059–7071. (b) Kendall, R. A.; Dunning, T. H.; Harrison, R. J. *J. Chem. Phys.* **1992**, *96*, 6796–6806.

(35) Yamada, S.; Morita, C.; Yamamoto, J. *Tetrahedron Lett.* **2004**, *45*, 7475–7478.

(36) For an overview on the DFT-D method, see: Grimme, S.; Antony, J.; Schwabe, T.; Mück-Lichtenfeld, C. *Org. Bio. Chem.* **2007**, *5*, 741–758, and references cited therein.

(37) (a) van Mourik, T. *J. Chem. Theory Comput.* **2008**, *4*, 1610–1619. (b) Pluháčková, K.; Grimme, S.; Hobza, P. *J. Phys. Chem. A* **2008**, *112*, 12469–12474. (c) van Mourik, T.; Karamertzanis, P. G.; Price, S. L. *J. Phys. Chem. A* **2006**, *110*, 8–12. See also: (d) Cohen, A. J.; Mori-Sanchez, P.; Yang, W. T. *Science* **2008**, *321*, 792–794.

(38) For a recent development in improving the charge transfer and related transitions, see: (a) Stein, T.; Kronik, L.; Baer, R. *J. Am. Chem. Soc.* **2009**, *131*, 2818–2820. (b) Ullrich, C. A. *J. Chem. Theory Comput.* **2009**, *5*, 859–865.

(39) Christiansen, O.; Koch, H.; Jörgensen, P. *Chem. Phys. Lett.* **1995**, *243*, 409–418.

(40) (a) Piacenza, M.; Grimme, S. *J. Am. Chem. Soc.* **2005**, *127*, 14841–14848. (b) Piacenza, M.; Grimme, S. *Chem. Phys. Chem.* **2005**, *6*, 1554–1558.

(41) For a recent overview of the PCM solvation method with the TD-DFT calculation, see: (a) Mennucci, B.; Cappelli, C.; Guido, C. A.; Cammi, R.; Tomasi, J. *J. Phys. Chem. A* **2009**, *113*, 3009–3020. See also: (b) Shivakumar, D.; Deng, Y.; Roux, B. *J. Chem. Theory Comput.* **2009**, *5*, 919–930.

(42) (a) Neese, F. *J. Biol. Inorg. Chem.* **2006**, *11*, 702–711. (b) Dreuw, A.; Weisman, J. L.; Head-Gordon, M. *J. Chem. Phys.* **2003**, *119*, 2943–2946. (c) Iikura, H.; Tsuneda, T.; Yanai, T.; Hirao, K. *J. Chem. Phys.* **2001**, *115*, 3540–3544. (d) Tozer, D. J.; Amos, R. D.; Handy, N. C.; Roos, B. O. *Mol. Phys.* **1999**, *97*, 859–868.

(43) (a) Grimme, S.; Parac, M. *Chem. Phys. Chem.* **2003**, *4*, 292–295. (b) Grimme, S.; Parac, M. *Chem. Phys.* **2003**, *292*, 11–21.

(44) Yamada, S.; Inoue, M. *Org. Lett.* **2007**, *9*, 1477–1480.

JP904243W